The International Journal of Advanced Manufacturing Technology (2024) 135:721–733
https://doi.org/10.1007/s00170-024-14531-6

ORIGINAL ARTICLE

Characterization of the heat transfer coefficient at near solidus forming condition using columnar pressing test

Muhammad Sajjad[1] · Julen Agirre[1] · Gorka Plata[1] · Jokin Lozares[2] · Joseba Mendiguren[1]

Received: 8 May 2024 / Accepted: 19 September 2024 / Published online: 1 October 2024

Abstract

This study addresses the significant gap in the literature regarding the heat transfer coefficient (HTC) under near-solidus forming (NSF) conditions, where materials are shaped close to their solidus state, presenting complex behaviour compared to traditional hot forming processes. Despite the pivotal role of heat transfer in developing a reliable material model for the digital twin (DT), limited data exist particularly regarding HTC characterization at NSF. Additionally, testing methodologies suitable for the high-temperature conditions, crucial for NSF processes, have not been adequately addressed. To fill this gap, this study aims to characterize HTC under NSF conditions using a columnar pressing test. The test was conducted at three different temperatures such as 1250, 1300, and 1360 °C and two different pressures, 2 and 8 MPa. During the test, temperature data was collected at the centre of the sample using a k-type thermocouple. Furthermore, the DT of the pressing test was developed and the three-dimensional finite element model of 42CrMo4 steel was constructed using FORGE NxT® 4.0 FEM software. The simulations were performed with varying HTC values to replicate the experimental test data. Inverse modelling techniques were then applied to compare experimental and simulated data, enabling the characterization and optimization of HTC values under NSF testing conditions. The results demonstrated that HTC in the NSF process is primary impacted by the forming pressure, whereas temperature change showed no variation at the studied ranges. The HTC value of 500 W/m^2K and 800 W/m^2K was identified at 2 MPa and 8 MPa, respectively. The conclusion of this study aims for a better understanding of heat transfer phenomena in NSF processes, enhancing the reliability of DT for industrial applications.

Keywords Near solidus forming (NSF) · Digital twin (DT) · FORGE NxT® 4.0 · Heat transfer coefficient (HTC)

1 Introduction

The near solidus forming (NSF) process, which involves materials forming close to their solidus state, has emerged as a promising technique in metal forming. Leveraging high ductility and excellent mechanical properties [1], this method presents an ideal solution for manufacturing complex geometries at the industrial scale, while minimizing material waste and energy consumption [2]. The digital twin methodology can be used to replicate the deformation behaviour of the NSF process and optimize it to increase efficiency and reduce CO2 footprint. However, the state-of-the-art NSF modelling does not account for reliable heat transfer coefficient characterizations and modelling. The heat transfer coefficient (HTC) governs the heat dissipation from the workpiece to the forging dies, and therefore it is critical for the correct representation of the process [3]. The heat transfer occurs at the interface between the workpiece and the tool, and it is typically described by the interface

✉ Muhammad Sajjad
msajjad@mondragon.edu

Julen Agirre
jagirreb@mondragon.edu

Gorka Plata
gplata@mondragon.edu

Jokin Lozares
jokin.lozares@deusto.es

Joseba Mendiguren
jmendiguren@mondragon.edu

1 Mondragon Unibertsitatea, Faculty of Engineering, Mechanics and Industrial Production, Loramendi 4, Mondragon 20500, Gipuzkoa, Spain

2 University of Deusto, Department of Mechanics, Design and Industrial Management, Avda. Of Universities 24, 48007 Bilbao, Spain

heat-transfer coefficient described by Boer et al. in the hot upsetting process[4]. The effect of HTC on the metal forming processes is not new; already in 1990, Burte et al. stated that the HTC was a critical parameter in the hot forging process [5]. In the nineteenth century, the Industrial Revolution catalyzed a deeper exploration of heat transfer principles, significantly impacting metal forming practices.

During the latter half of the twentieth century, there was a simultaneous acceleration in experimental techniques, as highlighted by Bergman et al. [6]. Innovations such as infrared thermography, thermocouples, and heat flux sensors revolutionized the field by enabling precise measurements and analyses of heat transfer during metal forming processes [7]. These advancements played a pivotal role in validating and refining theoretical models, effectively bridging the gap between empirical observations and scientific understanding.

One of the significant outcomes of this advancement was the rise of high-temperature forming processes. With further development in specialized alloys and technological breakthroughs, high-temperature forming processes gained popularity [8]. Techniques like hot forging, hot rolling, hot extrusion, and NSF, involving working metals at elevated temperatures, emerged. These methods allowed for enhanced formability, reduced forming forces, and improved control over material properties [9]. Understanding and optimizing heat transfer in these high-temperature processes became paramount, influencing product quality, efficiency, and cost-effectiveness in the manufacturing of metal components [10]. Despite the detailed investigation of HTC in other forming processes at elevated temperatures such as Malinowski et al. in the bulk metal forming process [11] and Baoshan et al. in the upsetting test of TC11 titanium alloy [12], the characterization of heat transfer in NSF has been largely overlooked (due to the challenges faced during NSF process, which includes high-temperature measurement, non-uniform heating, transient behaviour, material properties, heat losses, and finally testing methodology and measurement techniques).

To characterize heat transfer and validate models in high-temperature forming processes, various tests have been developed. These include tension, torsion, shear, and compression tests, as utilized by authors such as Piao et al. for tension/compression testing of AZ31B sheets and Johnson et al. [13, 14]. Each test variation has its own advantages and limitations, extensively explored by researchers in various studies [15]. The compression test for instance, involves rapidly compressing a cylindrical metal specimen between flat dies, leading to significant heat generation due to plastic deformation. This test was introduced by Dieter et al. in 1976 [16] and provides crucial data for understanding the heat transfer coefficient under specific deformation conditions. Nevertheless, the plastic work generates heat which is difficult to uncouple from the transfer and heat generation. In addition to experimental tests, other characterization methods such as inverse heat conduction methods and numerical simulations complement these tests, offering a comprehensive understanding of heat transfer in the high-temperature metal forming process [17]. Effective control of temperature gradients and heat flow at elevated temperatures significantly impacted the shaping of metals and continues to be a critical area of research and development in the field of metal forming [18].

In the literature, the columnar pressing test is a popular method for the characterization of heat transfer, due to its simplicity and ability to explore large ranges of strain and strain rate at high temperatures. Mendiguren et al. used the test to investigate the influence of the contact pressure and die temperature on the heat transfer coefficient employing USIBOR1500P material [19]. Similarly, Sethy et al. used the test to conduct the research on press velocity, HTC, processing time, mesh size, material, and tool temperature for Ti65 during high-temperature forming [20]. Later she performed the same test to characterize the HTC at high temperatures without deforming the billet [21].

From the literature, it is clear that heat transfer plays a critical role in the development of reliable material model as stated by Zhang et al. [22]. However, there is limited data available on the forming process, particularly under NSF conditions where the material is shaped close to its solidus state described by Lozares and Plata et al. in the manufacturing of NSF industrial components [1, 2]. Given the complexity of material behaviour in NSF compared to hot forging, there exists a significant gap in the literature concerning the characterization of heat transfer coefficients [23].

To address this gap, this study aims to characterize the HTC under NSF conditions through the columnar pressing test. The test was conducted at three temperatures: 1250, 1300, and 1360 °C, and under two different pressures: 2 and 8 MPa. Subsequently, a three-dimensional finite element model of 42CrMo4 steel for the pressing test was constructed using FORGE NxT® 4.0 FEM software. Simulations were conducted with varying HTC values to determine the temperature data under different temperature and contact conditions. Next inverse modelling techniques were employed to compare the experiment data with the simulation curves. Finally, the values of the HTC at NSF testing conditions are characterized and optimized. Overall, results showed that HTC remains stable across all temperature conditions however demonstrates significant change with contact pressure. At 2 MPa, the HTC value of 500 W/m^2K was concluded across all test conditions. Likewise, at higher contact pressures of 8 MPa, the HTC value is determined as 800 W/m^2K. The characterization of HTC at NSF conditions is pivotal for the accurate development of the NSF digital twin (DT), hence advancement towards the industrialization of the NSF process.

2 Research methodology

2.1 Sample preparation for the test

The material used in this study is a highly industrially used 42CrMo4 steel in the form of 20 mm diameter bars. For the experiments, billets of 20 mm±0.1 mm in height were extracted from the bar, maintaining the initial 20 mm in diameter, see Fig. 1.

For measuring the temperature profile during the experiments, a hole was drilled at the centre of the billet through electric discharge machined (EDM), positioned 10 mm away from the die's contact surface, as illustrated in Fig. 1. This cavity was designed to hold a K-type thermocouple with a diameter of 2 mm, extending to a depth of 10 mm. The use of a specially designed high-response K-type thermocouple from [11] facilitates the accurate temperature measurement throughout the experiment. Later, the temperature data will be used to predict the HTC values in these experiments.

2.2 Preparatory steps before the test

It is important that the thermocouple is fixed at a single point throughout the experiment to accurately measure the temperature at one point (billet centre). For this purpose, a light mechanical joint was generated through a sharp pointy tool as shown in Fig. 2a. Furthermore, in order to mimic the industrial process in which the dies are heated to reduce the heat lose, the dies were preheated with the help of a Hasco carbide heater as shown in Fig. 2b. For this purpose, a set of 230 V and 630 W die heaters, one at the top and one at the bottom die were installed in the preformed holes of the dies. To accurately control the temperature from the Hesco controller, a thermocouple was installed in both dies, which provided a real time temperature data throughout the experiment process.

2.3 Description of the test apparatus

In this study, a tooling arrangement was mounted onto a high-precision 40 kN SCHMIDT micro servo-press testing apparatus (detailed in Fig. 3). The dies were consistently kept at a temperature of 250 °C with the help of Hasco cartridge die heaters. The specimens were heated to the desired temperature in a Hobersal CRN-5X/17 electrical furnace. Before transferring the billet from the furnace to the press die, a CeraSpray® lubricant was sprayed onto the dies following the same strategy as in the industrial NSF process. This served to minimize the friction and to reduce

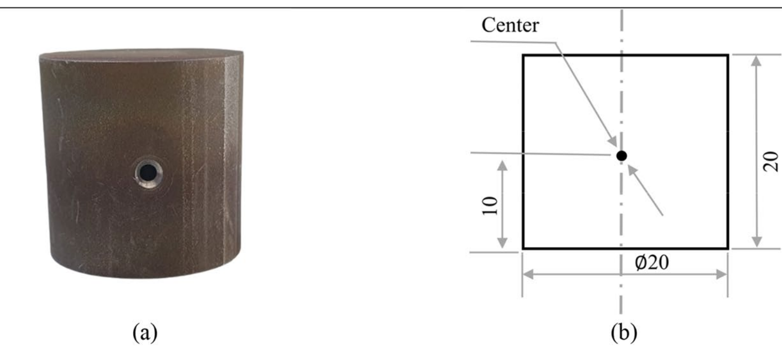

Fig. 1 Specimen geometry and thermocouple locations: **a**) Test sample, **b**) Sample specification (all units are in mm)

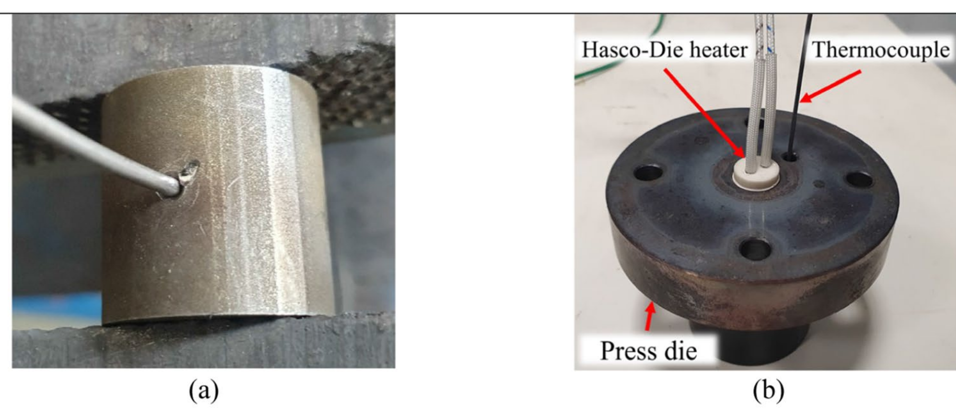

Fig. 2 Preparatory Steps: **a**) Mechanical welding of thermocouple, **b**) Press die with Hesco heater and thermocouple

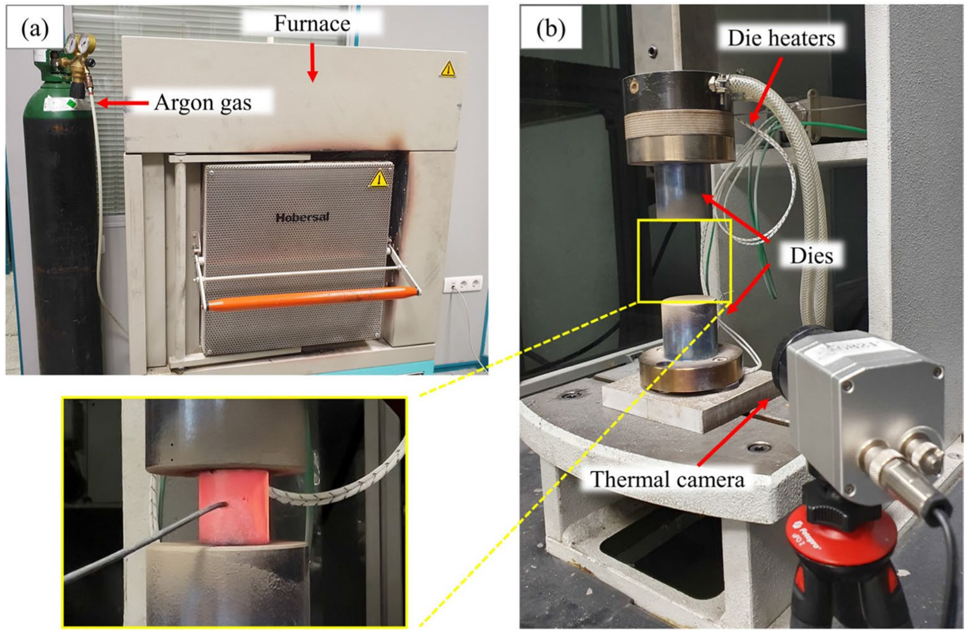

Fig. 3 Test setup: **a**) Furnace equipped with argon gas, **b**) Micro servo-press with thermal camera

the heat loss to the dies. The test specimen was connected to a responsive K-type thermocouple, which is further connected to a National Instruments NI9215 module data logger which facilitates the capture of temperature trends from furnace heating all the way to the transfer and pressing phase. Furthermore, to prevent excessive oxidation on the surface of the billet during the heating, a controlled argon atmosphere was created inside the furnace, which can be seen in Fig. 3a. Moreover, to investigate the temperature profile of the billet surface, a thermal camera was implemented as shown in Fig. 3b.

2.4 Test procedure

Experimental trials were conducted under two distinct contact pressures: 2 and 8 MPa. The low value of 2 MPa was selected to estimate the HTC value during the initial stages of the NSF process (low pressure), while a contact pressure of 8 MPa was chosen as the maximum contact pressure without the deformation of the billet.

The experiments were conducted using a high-precision micro servo-press, which provides closed-loop control of the applied force throughout the testing process. To characterize heat transfer at a specific contact pressure within the interface, a theoretical force calculation was used, assuming a planar contact across the entire 20 mm diameter surface. This assumption led to the application of forces of 628.32 N and 2513.28 N to achieve contact pressures of 2 MPa and 8 MPa, respectively. Initially, the press operated in a displacement-controlled mode at a high speed, with the speed reduced just before contact. During the heat transfer test, the press was switched to a force-controlled closed-loop mode.

The specification of the testing conditions is summarized in Table 1. The test was conducted at three temperatures: 1250, 1300, and 1360 °C. However, at 1360 °C, the material began to deform at a pressure of 8 MPa due to its yield limit; therefore, high-pressure data is neglected at 1360 °C. At the beginning, the test specimens were heated to a desired temperature in a furnace with a holding time to homogenizing the temperature. Similarly, to heat up the dies the Hasco carbide die heaters were run for extra time intervals and after achieving the thermal equilibrium at both specimen and dies, the specimen was relocated to the press. Three specimens were tested at each condition.

At the press, a nominal dwell interval of 0.7 s was designated before the pressing phase, where the press initiates its displacement from the top dead centre with a velocity of 80 mm/s and just before reaching the billet the velocity of the press was reduced to 1 mm/s to avoid the high-speed impact of the die. In the pressing phase of the test, the billet was pressed and held for a duration of 30 s. At the same time, the temperature data were collected by the thermocouple

Table 1 Boundary conditions of the columnar pressing test

Billet temperature °C	Pressure MPa	Ambient temperature °C	Dies temperature °C	Lubricant Type
1250	2			
1300	-			
1360	-	20	250	CeraSpray®
1250	8			
1300	-			

throughout the process. The billets after the pressing test are shown in Fig. 4. Utilizing the temperature profile of the specimen as input, the inverse calculation for HTC will be implemented.

3 Experiment results

The results of the specimen heating process, transitioning from room temperature to the target temperatures of 1250, 1300, and 1360 °C, are presented in Fig. 5. In these plots, time is represented on the *x*-axis, while temperature is plotted on the *y*-axis. All the plots are presented in the form of a confidence band. The average line represents the mean value of the temperature at all test repetitions at that time interval. Each plot in Fig. 5 represents three different repetition of individual test conditions. It is evident that, regardless of the chosen temperature, the billet reaches the intended temperature within approximately 225 s (4 min). Following this, the billet was left within the furnace for a few minutes more to ensure even temperature distribution throughout its body.

Fig. 4 Test samples after the pressing test

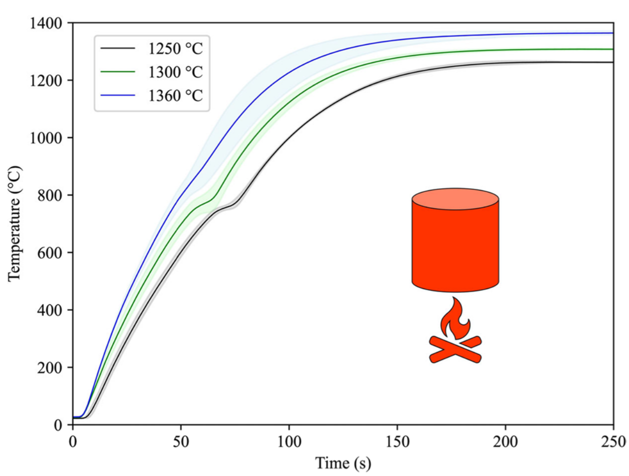

Fig. 5 Heating cycle of the billet inside the resistance furnace

Furthermore, it can be seen that at the initial stages, the billet heats up slowly for few seconds, which is due to the fact that the thermocouple was placed at the centre of the billet and initially the temperature of the furnace is redistributing in the billet causing slow heating. After this initial stage, the billet's temperature rises linearly until it reaches ~ 730 °C. At this point, a decline in temperature is observable due to microstructural changes. Subsequent to this phase, the material's temperature continues to rise until it ultimately reaches the intended target temperature.

Next, the plotted data illustrated in Fig. 6 shows the temperature change in the specimen throughout the columnar pressing test. Similarly, here all the plots are at three temperatures and two different pressures, with repetitions based on the boundary conditions shown in Table 1. The whole test is divided into three stages, labelled as (I), (II), and (III). Label (I) shows the time window in which the billet reached its targeted temperature and was still in the furnace (inside the furnace). Label (II) represents the time window in which the workpiece was moved from the furnace to the lower die (transfer phase). Finally, (III) shows the pressing phase, where the workpiece is pressed and held for 30 s.

Taking a closer look at each of the three phases, we can observe some interesting temperature changes. When the specimen was transferred from the furnace to the die, the temperature decreased by around 150 to 160 °C (in the centre of the billet where the thermocouple is measuring). Before the top die began moving down to press the specimen, at this point there was no external pressure on the test sample. Hence, the heat transfer coefficient was also low, leading to relatively minor heat transfer from the specimen to the die. However, the heat transfer increases during the pressing phase, as pressure builds up at the interface between the dies and the specimen when they come into contact. This facilitated rise in the heat transfer, which continued for 30 s as shown in Fig. 6 (all plots). This significant increase in the heat transfer coefficient linked to the applied pressure at the interface was discussed by Lu et al., during their investigation of the interfacial heat transfer coefficient for TC11 titanium alloy [12]. Furthermore, the increase in the heat loss is different for both pressures; for 2 MPa at all temperatures, we see a temperature loss of around 330 °C from the start to the end of the pressing phase, whereas in case of 8 MPa, the loss of 440–450 °C can be noted.

By looking deep into the individual plots, first, we see that in few experiments, the confidence band of the transfer phase is a bit wider compared to the rest of the phases. This is evident in Fig. 6a, which indicates a minor deviation in temperature during the transfer phase during the test caused by a slight rotation of the thermocouple attached to the centre of the billet. Also, the duration of the transfer phase is different in some cases, such as 15 s for 1250 °C at 2 MPa or 11 s for 1360 °C at 2 MPa. The minor delay was caused by

Fig. 6 Cooling phases of the test at different temperatures and pressure conditions

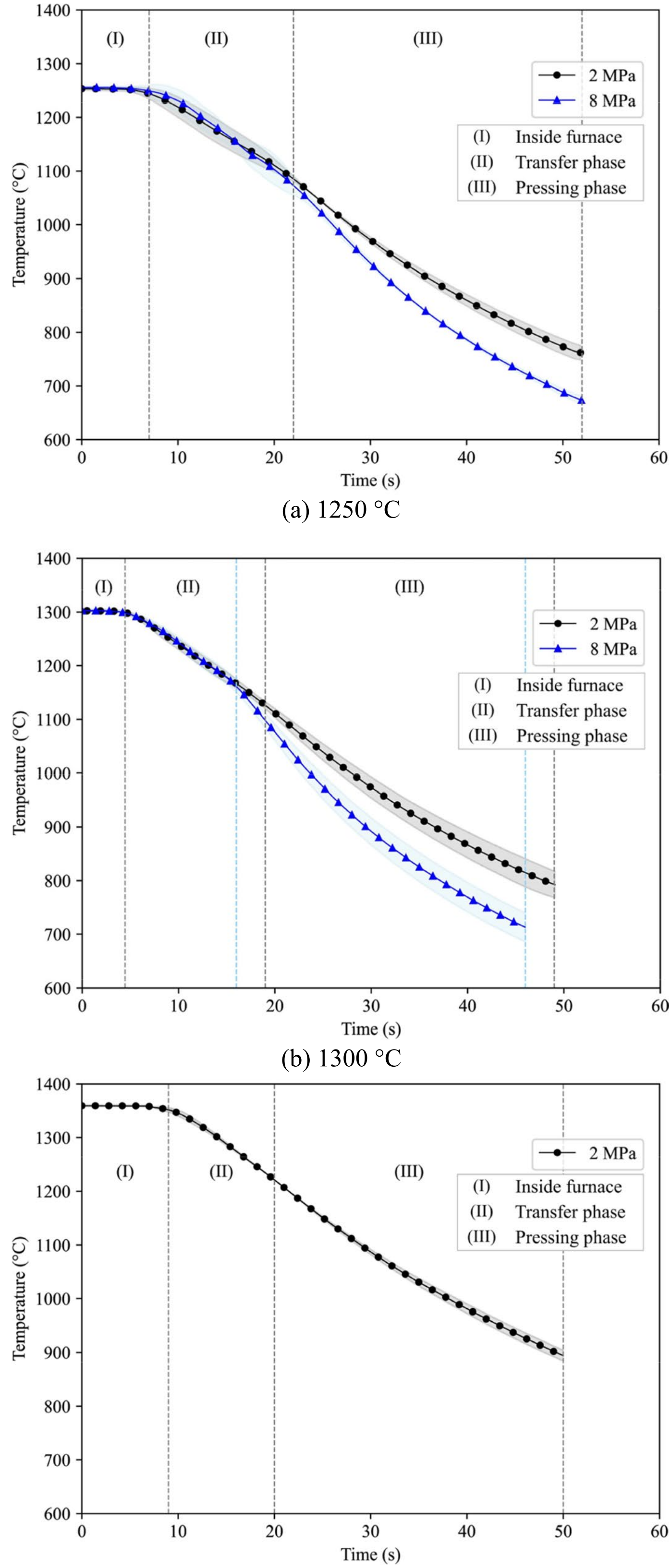

(c) 1360 °C

the placement of the billet, as the billet is attached to a thermocouple and sometimes the readjusting of the billet into the die's centres can cause a small variation in transfer time.

Overall, during all experiments, the billet was carefully transferred to minimize human errors as much as possible.

Figure 7 illustrates the thermal analysis of the test at a temperature of 1250 °C, utilizing the equipment as previously depicted in Fig. 3b. The figure is further divided into four sub figures: (a) showcasing the heated dies before the test, (b) representing the placement of the billet inside the press, (c) depicting the pressing phase, and (d) displaying the end of the pressing phase with the top die returning to its original position.

Figure 8 shows the thermal camera data at both 2 and 8 MPa at the temperature of 1250 °C. With readings taken at the billet's surface during the test, each graph is consisted of three repetition such as tests #1, #2, and #3. In Fig. 8a and b, the temperature curves differ for each test due to the variations in the transfer phase duration during the test. As the surface of the billet is more sensitive to heat dissipation into the air, shorter or longer transfer times could lead to different initial surface temperatures at the beginning of the pressing phase, even if they all show a similar trend for each repetition during the pressing phase.

However, despite having almost identical temperatures at the beginning, the pressing phase in 2 MPa ends at 652 °C while in 8 MPa it ends at 595 °C (Fig. 8). Which clearly indicates the effect of pressure on the heat transfer coefficient during the NSF process. Overall, the thermal camera analysis demonstrated similar heat transfer behaviour compared to the thermocouple data.

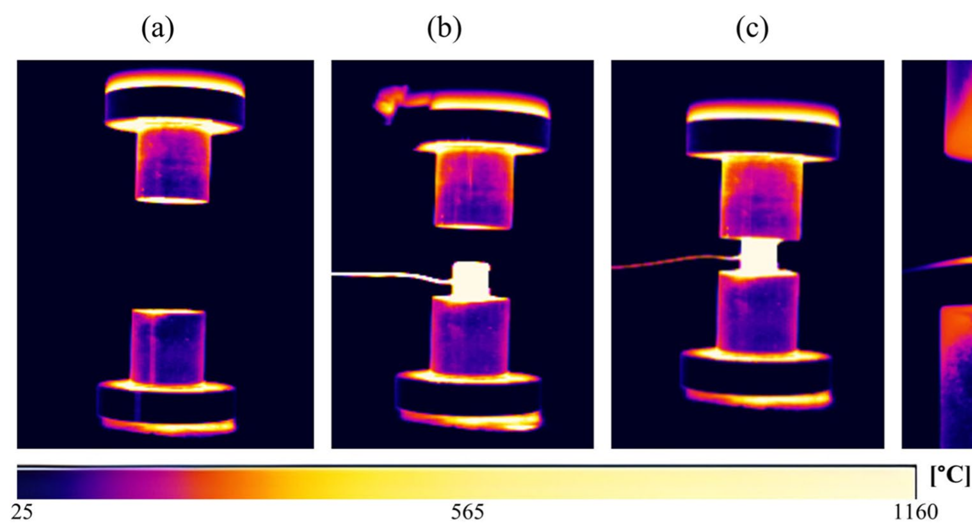

Fig. 7 Thermal camera analysis: **a**) heated dies, **b**) billet placement inside press, **c**) pressing phase, **d**) post-pressing phase

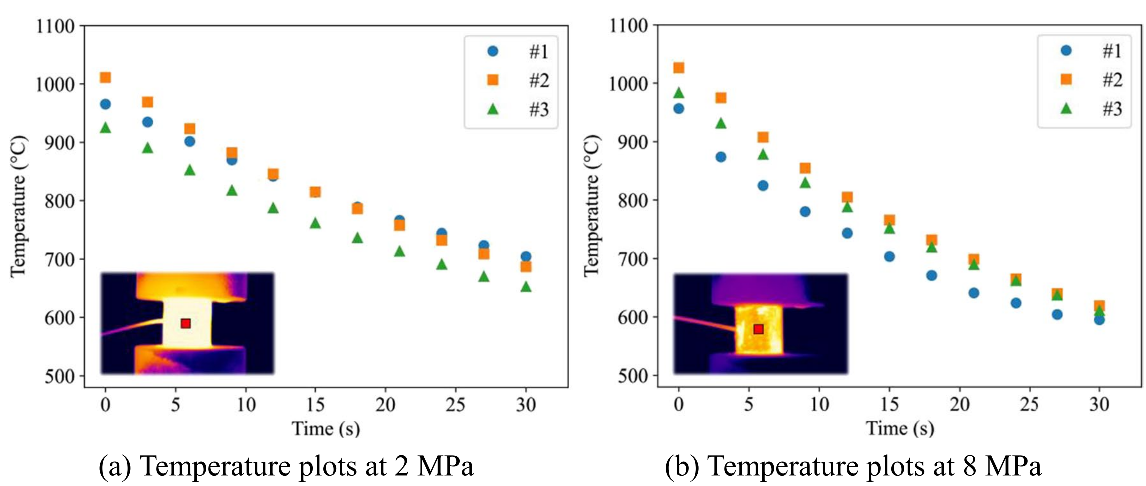

Fig. 8 Thermal camera temperature data at 1250 °C

4 Methodology, model generation, and the calculation of HTC

4.1 Inverse analysis methodology

To calculate the HTC, reverse analysis was implemented, and its details can be seen in Fig. 9. For this purpose, a comprehensive DT model was developed to replicate the experimental process depicted in Fig. 6, which consists of the transfer phase, dwell time, and pressing phase. The DT is focused particularly on understanding the temperature dynamics during these phases, with the transfer phase influenced significantly by heat exchange to air (HEA), and the pressing phase by the heat transfer coefficient (HTC). To thoroughly investigate these dependencies, the simulations study was conducted with a wide range of HTC and HEA values. With this approach, the thermal behaviour of the sample during the experiment trials can be replicated. Through deep analysis, the evolution of temperature profiles for each simulated scenario was tracked. Subsequently, aligning experimental temperature data with these numerical predictions enables a precise comparison between simulated and observed outcomes. This methodology enabled us to identify the specific HEA and HTC values that accurately reproduce the temperature profiles observed in experimental trials.

4.2 Numerical modelling

The implementation of heat transfer laws in various software platforms may introduce slight disparities. Consequently, it was essential for the authors to perform inverse calculations of transfer coefficients using the same software utilized in industrial forming simulations. Notably, FORGE NXT® stands out as one of the most commonly employed software tools for this purpose. This numerical analysis tool excels in simulating large strain thermo-plasticity deformation behaviour, making it a preferred choice for industrial forging and numerical simulation framework (NSF) applications. In this study, a 3D finite element model of 42CrMo4 steel for the pressing test was meticulously crafted using the FORGE NXT® finite element software to facilitate the development of the desired transfer coefficients. For the plastic behaviour of the material, the Hansel–Spittel model, which describes the relationship between flow stress, strain, strain rate, and deformation temperature is used. The Hansel–Spittel model is expressed by the following equation

$$\sigma = Ae^{m_1 T}\varepsilon^{m_2}\dot{\varepsilon}^{m_3}e^{\frac{m_4}{\varepsilon}}(1+\varepsilon)^{m_5 T}e^{m_{7\varepsilon}}\dot{\varepsilon}^{Tm_8}T^{m_9} \tag{1}$$

In this context, σ represents stress, ε denotes strain, $\varepsilon^{\cdot}$ is the strain rate, T is the deformation temperature, and m_1 to m_9 are material constants. The boundary conditions used in the simulations are summarized in Fig. 10a. The upper and lower tools were represented as rigid entities, with the unilateral contact and the friction coefficient at the part/die interface. For which the Coulomb limited Tresca model is implemented from the FORGE database, details of which can be found in the paper [23]. The heat transfers were established between the parts and dies, as well as between the parts and the surrounding air. The HTC is governed by the transient heat conduction equation known as Fourier's law; a mathematical form of the equation is expressed:

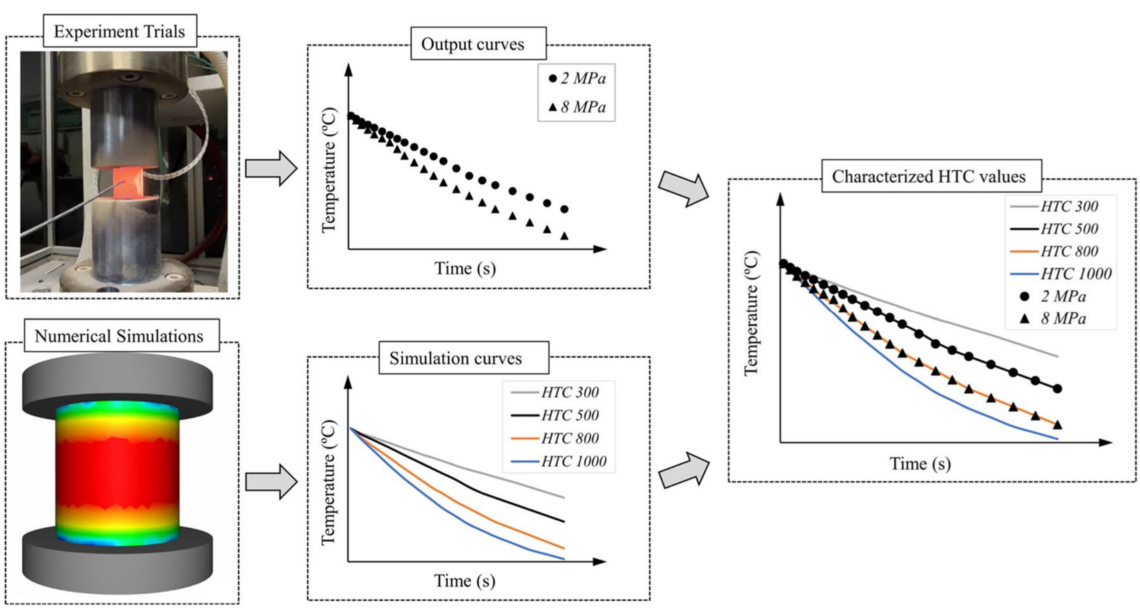

Fig. 9 HTC characterization process flow chart

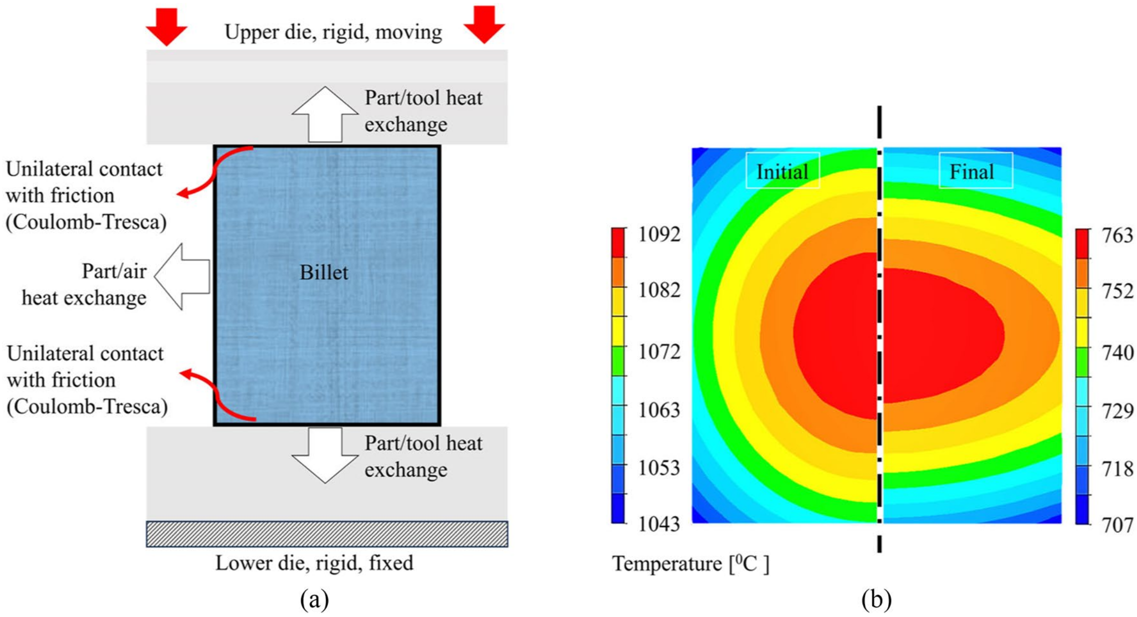

Fig. 10 Numerical modeling of the columnar pressing test: **a**) boundary conditions, **b**) temperature distribution during the test

$$\frac{\partial T}{\partial_t} = \alpha_d \left(\frac{\partial^2 T}{\partial x^2} \right) \tag{2}$$

where T represents the temperature, t is time, x is the space variable, and the material properties are introduced by α_d that it is defined as

$$\alpha_d = \frac{k_d}{\rho_d c_d} \tag{3}$$

where k_d is the thermal conductivity, ρ_d represents the density, and c_d is the specific heat. While the lower die remained stationary, a predetermined vertical displacement was imposed on the upper die. In the simulation, the dies were assigned temperatures of 250 °C, with the surroundings air temperature (20 °C). The specimen was partitioned into 36,360 tetrahedron elements with 7369 nodes, while the dies were kept as a rigid body. The resulting average mesh size of the billet was ~ 0.7 mm throughout the process. For the press, the experimental force of 2 or 8 MPa for each experiment was imposed on the corresponding simulation. Furthermore, the remeshing rule was implemented in the simulation to reduce the computational time while increasing the accuracy of the simulation results.

To include the initial heterogeneous temperature distribution observed during the experiment test, the simulation process consisted of three main stages. In the first stage (I), the temperature evolution is determined during billet transfer from the furnace to the press table while employing the exchange of heat with air along the billet's entire boundary surface. In the second stage, (II) the temperature evolution is simulated for the period when the billet was placed on the press die, while the billet deformation is not commenced. Finally, the upper die was subjected to a predefined contact pressure (III), pressing the specimen between the upper and lower die at the desired pressure. Throughout the simulation, the temperature history of the specimen was monitored using a virtual sensor situated at the centre of the billet similar to the experiment test. The process times for the first two stages replicated the experimental data.

Figure 10b graphically illustrates the temperature gradients in a typical pressing test for 42CrMo4 at 1250 °C, prior and after the pressing. Overall, it can be seen that at 1250 °C, approximately a temperature of 158 °C was lost during the transfer phase. Furthermore, the highest temperature can be noticed at the centre of the billet whereas the surface is cooler due to higher heat loss to the air, as shown in Fig. 10b.

Overall, the simulation was carried out defining different values of the HTC which resulted in different temperature evolutions at the centre of the billet. By comparing both experiment and simulation curves, the correct HTC value was optimized and minimized for the pressing test (Fig. 9).

4.3 HTC calculations analysis

Figure 11 illustrates the inverse identification procedure as depicted in Fig. 9. The experimental temperature evolution at the centre of the billet is denoted by black dots (2 MPa) and blue triangles (8 MPa) markers. Additionally, the continuous lines represent the temperature evolution prediction by the digital twin (DT) under various assumed heat transfer coefficients (HTC). Notably, for the scenario of 2 MPa pressure, a HTC of 500 W/m^{2}K is found to accurately reproduce the temperature evolution. Conversely, under high contact pressure conditions (8 MPa), a higher HTC of 800 W/m^{2}K is necessary to match the experimental heat loss.

As presented in Fig. 6, during the second phase (II), the heat loss is controlled by the heat exchange to air (HEA) coefficient. Therefore, the same procedure as the one just presented can be used to characterize the HEA considering phase two (II) experimental data. As in the transfer phase, the billet was in contact with the air and the transfer tool, the heat was lost due to conduction, convection, and radiation; hence, the cooling curve for 2 and 8 MPa testing is considered as multiple repetitions of the same test.

In Fig. 12, the output of the inverse analysis conducted for the three different experimental temperatures, the different contact pressures, and both transfer phase (II) for HEA identification and phase three (III) for HTC identification are presented.

At 1250 °C, the cooling rate was recorded around 10 °C/s during the transfer phase (Fig. 12a). In the pressing phase, the heat loss is accentuated due to the transfer from the billet to the dies. At a window of 30 s, the temperature at 2 MPa is declined by ~ 320 °C, whereas for high pressure 8 MPa, this decline is ~ 400 °C, shown in Fig. 12b.

Similarly, at 1300 °C, as shown in Figs. 12c and d, there is a notable alignment between the experimental and simulated curves. At this temperature, the cooling rate is calculated to be approximately 13.5 °C, representing a 3.5 °C increase compared to the cooling rate at 1250 °C. This observation suggests that heat loss is more pronounced at higher temperatures and, conversely, lower at lower temperatures.

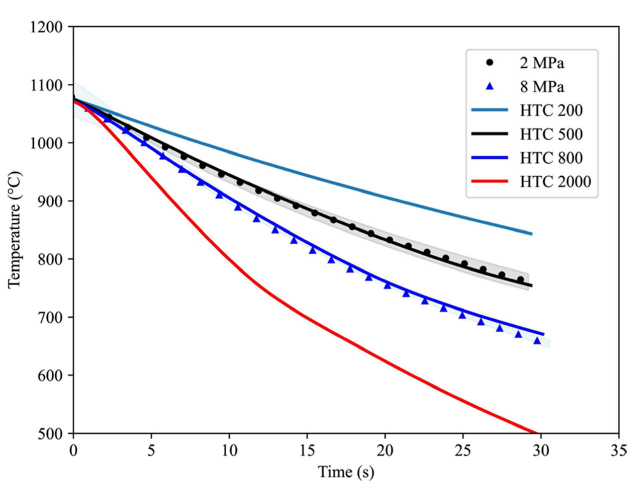

Fig. 11 Comparison of numerical and experimental results at various HTC values

Examining the pressing phase plots, in the case of 2 MPa, the temperature decreases from an initial temperature of 1133 °C to approximately 800 °C, while for 8 MPa, the final temperature is recorded at around 690 °C at the end of the pressing phase. This reflects a temperature drop of 110 °C compared to the low-temperature condition (1250 °C). Furthermore, the disparity in heat loss between 2 and 8 MPa is notably greater compared to 1250 °C, attributed to the higher temperature profile.

Finally, Figs. 12e and f depict the correlation of temperature profiles between experimental and simulation tests at 1360 °C. These plots illustrate the model's accurate prediction of the transfer phase, as depicted in Fig. 12e. Moreover, at 1360 °C, the cooling rate initiates at approximately 15 °C/s, gradually decreasing to 13 °C/s by the end of the transfer phase (from around ~ 1220 to ~ 907 °C). This highlights the significant influence of sample and surrounding air temperatures on the cooling rate, which increases with higher temperatures and decreases vice versa. This trend is evident when comparing the cooling rates at 1250, 1300, and 1360 °C. Additionally, in the pressing phase, the model effectively predicts the temperature curve from the beginning to the end of the pressing phase, as shown in Fig. 12f. However, no reliable experiment data was obtained at 1360 °C under contact pressure of 8 MPa due to material limitations.

The characterized heat exchange to the air and heat transfer coefficient under NSF conditions are summarized in Fig. 13. Figure 13a illustrates the relationship between HEA and the initial transfer temperature, while Fig. 13b displays the characterized HTC under various contact pressures and temperatures.

On one hand, the conducted study reveals a minor dependency of the HEA on the transfer temperature, with a slight coefficient increase observed as the transfer temperature rises. On the other hand, the HTC appears to remain stable across the tested temperature range but demonstrates significant dependency on contact pressure.

Overall, in this study, the HTC exhibited only a minor dependency on temperature within the specific temperature range and investigated experimental conditions. This finding is consistent with certain conditions where the influence of temperature on HTC is not pronounced, such as in scenarios where the surface characteristics or contact conditions dominate the heat transfer behaviour. In this study, we focused on a relatively narrow temperature range (1250 to 1360 °C) compared to the broader temperature ranges examined in some other literature studies.

However, in other contexts, particularly under different material conditions, surface roughness, oxidation, or higher temperature ranges, the HTC can show a significant dependency. For instance, literature reports variations in HTC with temperature due to factors such as phase changes at the interface, changes in material properties like thermal

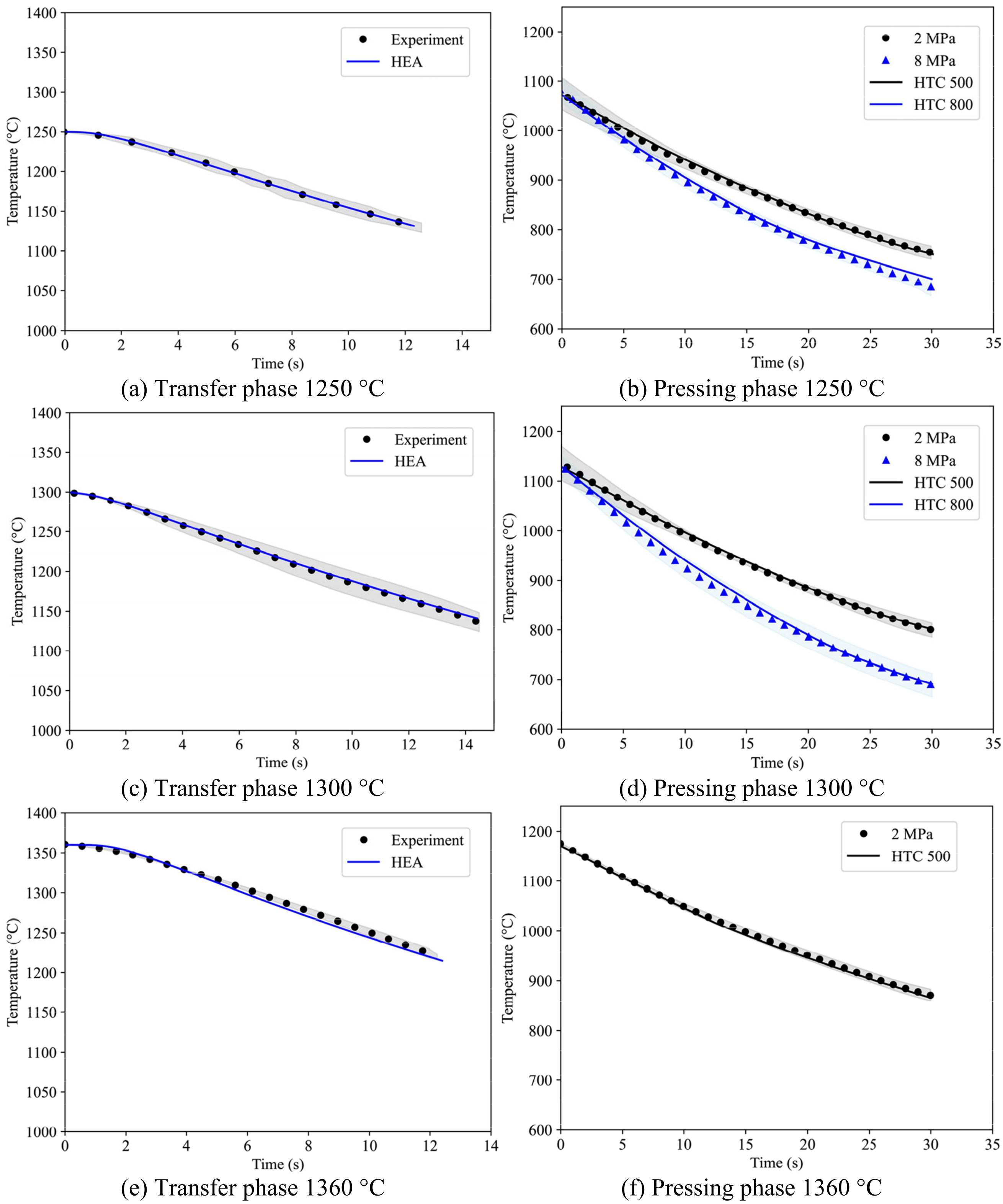

Fig. 12 Comparison of experimental and simulation data; transfer phase and pressing phase

conductivity, and variations in surface emissivity. For example, studies such as [24] have shown that in certain metal forming processes, the HTC increases with temperature due to enhanced thermal conductivity at higher temperatures or

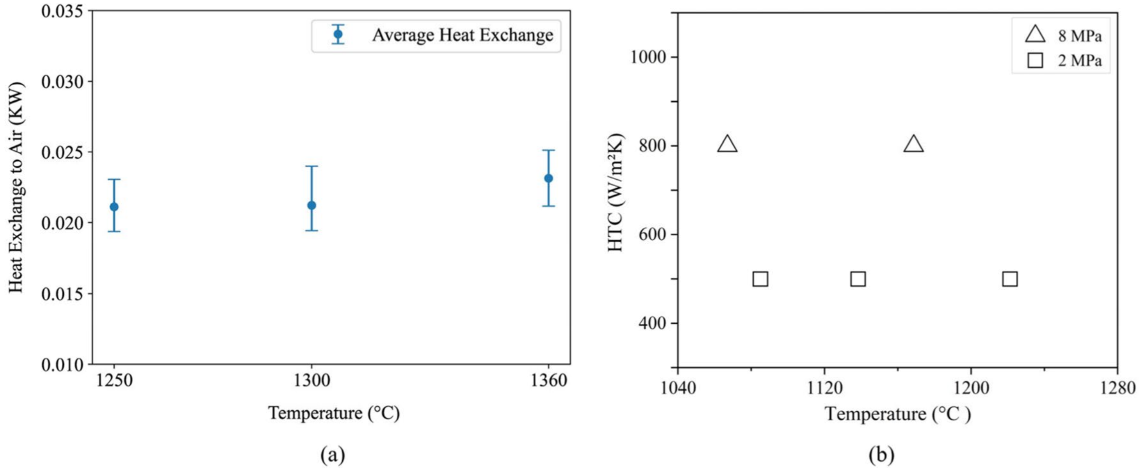

Fig. 13 Thermal analysis at all temperature conditions: **a**) heat exchange to air **b**) thermocouple temperature before pressing

changes in interfacial conditions. Conversely, other studies [25] have reported minimal dependency when the contact surfaces are relatively smooth, and the temperature range is narrow. Our findings suggest that within the specific range of near-solidus temperatures investigated, the HTC remains relatively stable. This could be attributed to the consistent contact conditions maintained during the experiments, as well as the specific material properties at the examined temperatures. However, we do not intend to generalize this observation beyond the scope of our study and further investigation is needed to address this in more detail.

5 Conclusion

The columnar pressing test is developed to calculate the HEA and HTC under NSF conditions for 42CrMo4 steel. For this purpose, tests were conducted at a temperature and pressure of 1250, 1300, 1360 °C, 2 and 8 MPa, respectively. A reverse analysis has been performed by comparing the experiment results with the simulation in FORGE NXT®. Based on the findings presented in this work, the following conclusions are drawn:

- A minor dependency of the HEA on the transfer temperature has been found.
- The HTC appears to remain stable across the tested temperature range but demonstrates significant dependency on contact pressure.
- At a low contact pressure of 2 MPa, a consistent HTC value of 500 W/m^{2}K was identified for all tests. Likewise, at higher contact pressures of 8 MPa, the HTC value remained at approximately 800 W/m^{2}K across all test conditions.

In summary, this study addresses the identified research gap by providing essential data on HEA and HTC under NSF conditions for 42CrMo4. These characterizations are pivotal for the accurate development of the NSF digital twin (DT) and, consequently, for the industrialization of the NSF process. However, it is important to note a limitation of the current study, which only investigates low pressures of 2 MPa and 8 MPa, allowing for the isolation of plastic work and HTC effects. Nonetheless, given the expectation of higher contact pressures during the NSF process, further investigations will be necessary to encompass the full range of industrial pressure scenarios.

Acknowledgements The authors would like to acknowledge the *Exploration of high entropy alloys as substitute materials for sustainable mobility and decarbonisation (HEAPLAS)* project funded by Ministerio de Ciencia e Innovación, with the reference PID2022-139130OA-I00, the HSSF, *Hybrid Semi-Solid Forming* project funded by the "Research Fund for Coal and Steel" (RFCS) program of the European Union, with the grant number 800763, and the *Procesos de Fabricación de Excelentes para propiedades máximas (PROMAX),* funded by Basque Government through the ELKARTEK funding scheme (reference KK-2020/00087).

Author contribution statement Muhammad Sajjad**:** methodology, investigation, software, formal analysis, validation, visualization, writing—original draft.

Julen Agirre: methodology, investigation, formal analysis.

Gorka Plata: conceptualization, methodology, investigation, writing—review and editing.

Jokin Lozares: conceptualization, methodology, investigation, writing—review and editing, resources.

Joseba Mendiguren: conceptualization, resources, supervision, project administration, writing—review and editing.

Funding Open Access funding provided thanks to the CRUE-CSIC agreement with Springer Nature.

Declarations

Author agreement We declare that this manuscript entitled "Characterization of the heat transfer coefficient at near solidus forming condition using columnar pressing test" is original, has not been published before, and is not currently being considered for publication elsewhere.

We confirm that the manuscript has been read and approved by all named authors and that there are no other persons who satisfied the criteria for authorship but are not listed. We further confirm that the order of authors listed in the manuscript has been approved by all of us. We understand that the Corresponding Author is the sole contact for the Editorial process. He is responsible for communicating with the other authors about progress, submissions of revisions, and final approval of proofs.

Declaration of generative AI and AI-assisted technologies in the writing process During the preparation of this work, the author(s) used Chat GTP Open AI 3.5 for the rewrite of the text to improve its quality. After using this tool, the author(s) reviewed and edited the content as needed and take(s) full responsibility for the content of the publication.

Competing interests The authors declare no competing interests.

References

1. Lozares J, Plata G, Hurtado I, et al (2020) Near solidus forming (NSF): semi-solid steel forming at high solid content to obtain as-forged properties. Metals (Basel) 10:. https://doi.org/10.3390/met10020198
2. Plata G, Lozares J, Sánchez A et al (2020) Preliminary study on the capability of the novel near solidus forming (NSF) technology to manufacture complex steel components. Materials 13:1–14. https://doi.org/10.3390/ma13204682
3. Chang CC, Bramley AN (2002) Determination of the heat transfer coefficient at the workpiece±die interface for the forging process. Proc Instn Mech Engrs Part B: J Engineering Manufacture B:1179–1186. https://doi.org/10.1243/095440502760272449
4. Boër CR, Schröder G (1981) Heat transfer during hot upsetting in heated dies. In: Proceedings of the Twenty-First International Machine Tool Design and Research Conference. Macmillan Education UK, London, pp 209–215
5. Burte PR, Im Y-T, Altan T, Semiatin SL (1990) Measurement and analysis of heat transfer and friction during hot forging
6. Bergman, Theodore L, Lavine, et al (2011) Introduction to heat transfer, 6th Edition. John Wiley & Sons
7. Vavilov V, Burleigh D (2020) Infrared thermography and thermal nondestructive testing. Springer International Publishing, Cham
8. Maikranz-Valentin M, Weidig U, Schoof U et al (2008) Components with optimised properties due to advanced thermomechanical process strategies in hot sheet metal forming. Steel Res Int 79:92–97. https://doi.org/10.1002/srin.200806322
9. Hosford, William F, Caddell, Robert M (2011) Metal forming: mechanics and metallurgy. Cambridge university press
10. Chang CC, Bramley AN (2002) Determination of the heat transfer coefficient at the workpiece—die interface for the forging process. Proc Inst Mech Eng B J Eng Manuf 216:1179–1186. https://doi.org/10.1243/095440502760272449
11. Malinowski Z, Lenard JG, Davies ME (1994) A study of the heat-transfer coefficient as a function of temperature and pressure. J Mater Process Technol 41:125–142. https://doi.org/10.1016/0924-0136(94)90057-4
12. Lu B, Wang L, Geng Z, Huang Y (2017) Determination of interfacial heat transfer coefficient for TC11 titanium alloy hot forging. Heat Mass Transf 53:3049–3058. https://doi.org/10.1007/s00231-017-2032-5
13. Piao K, Lee JK, Kim JH et al (2012) A sheet tension/compression test for elevated temperature. Int J Plast 38:27–46. https://doi.org/10.1016/j.ijplas.2012.03.009
14. Johnson GR (1981) Dynamic analysis of a torsion test specimen including heat conduction and plastic flow. J Eng Mater Technol 103:201–206. https://doi.org/10.1115/1.3225001
15. Pöhlandt K (1989) Materials testing for the metal forming industry. Springer, Berlin Heidelberg, Berlin, Heidelberg
16. Dieter GE, Bacon D (1976) Mechanical metallurgy. McGraw-hill, New York
17. Orlande HRB (2010) Inverse problems in heat transfer: new trends on solution methodologies and applications. In: 2010 14th International Heat Transfer Conference, Volume 8. ASMEDC, pp 379–398
18. Zhao K, Wang B, Chang Y et al (2015) Comparison of the methods for calculating the interfacial heat transfer coefficient in hot stamping. Appl Therm Eng 79:17–26. https://doi.org/10.1016/j.applthermaleng.2015.01.018
19. Mendiguren J, Ortubay R, De Argandonã ES, Galdos L (2016) Experimental characterization of the heat transfer coefficient under different close loop controlled pressures and die temperatures. Appl Therm Eng 99:813–824. https://doi.org/10.1016/j.applthermaleng.2016.01.133
20. Sethy R, Galdos L, Mendiguren J, Sáenz De Argandoña E (2016) Investigation of influencing factors on friction during ring test in hot forging using FEM simulation. In: AIP Conference Proceedings. American Institute of Physics Inc.
21. Sethy R, Galdos L, Mendiguren J, Sáenz de Argandoña E (2017) Friction and heat transfer coefficient determination of titanium alloys during hot forging conditions. Adv Eng Mater 19:. https://doi.org/10.1002/adem.201600060
22. Zhang L, Reilly C, Li L et al (2014) Development of an inverse heat conduction model and its application to determination of heat transfer coefficient during casting solidification. Heat Mass Transf 50:945–955. https://doi.org/10.1007/s00231-014-1304-6
23. Sajjad M, Trinidad J, Plata G, et al (2024) Sensitivity analysis of near solidus forming (NSF) process with digital twin using Taguchi approach. Adv Manuf
24. Lenard JG, Davies ME (1992) An experimental study of heat transfer in metal-forming processes. CIRP Ann 41:307–310. https://doi.org/10.1016/S0007-8506(07)61210-4
25. Zhang L, Yuan J, He S et al (2021) Contact heat transfer analysis between mechanical surfaces based on reverse engineering and FEM. Tribol Int 161:107097. https://doi.org/10.1016/j.triboint.2021.107097